LHCb Collaboration LHCB 00-051 CALO
September 10, 2000

On the possibility of *in situ* calibration of LHCb calorimeters

I.Korolko, V.F.Obraztsov, S.Popescu, O.P.Yushchenko
ITEP, Moscow, Russia
IHEP, Protvino, Russia
IFIN-HH, Bucharest, Rumania

Abstract

To investigate a possibility of *in situ* calibration of the ECAL and HCAL, the rates of isolated electrons and hadrons are estimated from LHCB standard MC data. Several possible algorithms of a fast calibration are tested to evaluate the minimal statistics required and to demonstrate the feasibility of the procedure.

1 Introduction

In this note we present the results of our studies on the possibility to calibrate the LHCb electromagnetic and hadron calorimeters, using experimental data collected by the proposed DAQ system. The main reasons of a proper calibration (relative cell-to-cell and absolute), for selective trigerring and efficient data analysis, are:

- The LHCb calorimetry is planned to provide an essential part ($\sim 80\%$ of allowed bandwidth) of all Level0 high E_T triggers. Moreover, energetic clusters found in both LHCb calorimeters and associated with track segments reconstructed in vertex detector, will improve the performance of the next level trigger algorithms, by reducing the number of fake secondary verticies.
- Reconstruction of different B-hadron final states and efficient tagging of initial b-quark flavor require reliable lepton identification. Precise ECAL measurements are used for electron (positron) identification in full momentum range.
- Monte-Carlo studies have demonstrated the ability of the LHCb detector to reconstruct B-hadron decay channels with photons and π^0s. Perfect ECAL calibration helps us to minimize the mass peak width of reconstructed particles (both B-mesons and π^0s) considerably reducing the background level.

In order to keep the resolution of the calorimeter at the required level, the whole chain, consisting of calorimeter cells, photodetectors and ADC's has to be calibrated and monitored. Several different types of calibration are foreseen for the calorimeters [1]:

1. Monitoring systems using pulsed light sources (for example LED's).
2. ^{137}Cs radioactive source driven hydraulically through the tubes in the HCAL body.
3. Charge injectors for the ADC's and trigger logic calibration.

This systems provide relative cell-to-cell calibration as well as the control of the time stability of the calorimeters. None of this methods gives the absolute energy calibration as well as the adequate information about the radiation damage of the active part of the calorimeters. To complement the above mentioned methods this note summarises the feasibility studies of the *in situ* calibration which uses the on-line real data flow from the experimental setup.

2 The calibration of the calorimeters using on-line experimental data.

The main idea of the method is to use particles (electrons for the ECAL, hadrons for the HCAL and muons for both calorimeters) with momenta measured by the tracking system. We do not specify the source of these particles, it can be b,c,s semileptonic decays, photons converted upstream of the LHCB magnet, processes with the internal photon conversion like $\eta \to e^+e^-\gamma$ etc.

There are several points in the data flow where this calibration can be done:

- Inside the Level-2 trigger.

- Inside the Level-3 trigger.

The first option is, of course, more attractive from the point of view of statistics. The expected data flow is $\sim$ 40 kHz at the Level-2 input. After the Level-2 the data flow is $\sim$ 5 kHz, but the quality of the data reconstruction is much better. It looks reasonable to foresee the calibration at both levels.

We will assume that Level-2 and Level-3 triggers will be based on a farm of commercial processors and that some part of them will be available for calibration purposes.

Extremely high energies of the proton-proton collisions at LHC and forward geometry chosen for the LHCb spectrometer will produce a rather intensive flux of particles (e,h,π^0) to be observed in the calorimeter system. The LHCb trigger selects events with B-hadrons decaying in detector acceptance and therefore increases the flux of useful particles. All subsequent results presented in this note are given for $b\bar{b}$ events accepted by these two trigger levels. We assume that next trigger levels selecting particular B-decay modes would not change particle yields too much. We have also assumed that MinBias events passed through the first two trigger levels would have very similar multiplicities.

Another important issue we are trying to cover in this note - is our ability to calibrate calorimeters during the very first days of LHC operation. In a most pessimistic scenario we are assuming that data from all other LHCb sub-detectors are unavailable. Our aim is to demonstrate that even in a worst situation we can calibrate our devices but of course with a limited accuracy.

3 ECAL calibration System

The transverse granularity and dynamic range of the LHCb electromagnetic calorimeter where optimized for B-physics needs and are shown in Table 1. In total our calorimeter consists of 5952 channels. The gain and linearity of each channel have to be calibrated independently taking into account the following:

- The characteristics of front-end electronics (PMs parameters, HV supply, noise level) may be different.

- The properties of "shashlik" modules (plastic plates, fibres, optical contacts) are not exactly the same.

- The expected radiation doses and corresponding performance degradation strongly depend on the distance from the beam pipe.

Moreover, the parameters of the calorimeter channels may vary with time, therefore it is desirable to collect data for calibration within a reasonably short time period.

The proposed ECAL calibration scheme satisfying all mentioned requirements includes the following steps:

1. Pedestals determination for all calorimeter channels, which is done on-line, analysing signals from two previous events as described in [2]. We also foresee possibility to

ECAL section	**Inner**	**Middle**	**Outer**
Cell size	40.4 mm	60.6 mm	121.2 mm
Dimensions	198.72 × 149.04 cm	397.44 × 248.40 cm	794.88 × 645.84 cm
No. of channels	1472	1792	2688
Dynamic range, E_t	0 - 10 GeV	0 - 10 GeV	0 - 10 GeV
ADC	12 bits	12 bits	12 bits

Table 1: Parameters of the LHCb electromagnetic calorimeter.

have special “pedestal runs”. The width of pedestals distribution (~ 1 ADC bin) may have the same effect on the measurement of low energy particles as intrinsic “shashlik” resolution.

2. The stability-monitoring system correcting for possible time-dependent gain variations as described in [3]. Two monitoring techniques, based on the use of either multiple LED assemblies or a high intensity nitrogen laser, are under study. Such a system will also allow to transfer the test beam calibration of a subset of modules during production phase to the rest of the modules at startup. Another attractive task of monitoring system is to determine the linearity of PM gain for each calorimeter channel varying the light amplitude. (However it requires proper calibration of light sources)

3. Calibration of the whole calorimeter with experimental data. Several techniques, covering the full dynamic range and using different subsets of sub-detectors , were considered:

   - Rough pre-calibration with energy flow measurements. Distributions of energy depositions in the whole ECAL, with a good statistics, can be collected within a few seconds of detector operation, providing robust on-line monitoring tool.
   - Monitoring of ECAL performance at very low energies with MIPs. Sufficiently large data samples can be collected (for every cell) within ~ 5-10 minutes of LHCb operation. It can be used for control of the calorimeter time stability also.
   - Precise ECAL calibration at intermediate energies with electrons (resulting mainly from photon conversion on the material before the magnet) within ~ 20-40 minutes of data taking.
   - A special π^0 calibration is foreseen for the first days of the LHCb operation when (in a worst scenario) no momentum measurements from the tracker would be available.

3.1 Energy Flow measurements

This method utilizes the fact that energy flow measured with ECAL should depend smoothly on the distance from the beam pipe. Using 400K inclusive $b\bar{b}$ events, generated with PYTHIA and pathed trough the full GEANT simulation of our detector, we have obtained 2-dimensional distributions of energies (in terms of E_t) deposited in ECAL cells. The corresponding distribution for inner ECAL section is shown in Figure 1. We have not taken into account trigger for these particular studies assuming that it would not change smooth behavior of the transverse energy flow distributions. In this assumption, 400K events corresponds to 10 seconds of normal LHCb operation if we are able to collect data on Level2.

The demonstrated smooth dependence is destroyed in real detector by poor knowledge of relative calibration constants in neighbour channels. Assuming $\pm 30\%$ uncertainties in relative calibration over the whole calorimeter, we have multiplied energies accumulated in every cell with a constants RMC_{ij} (i-column, j-row numbers) distributed uniformly within [0.7 - 1.3] range. Then we have smoothed "de-calibrated" distributions with a standard multiquadratic algorithm described in [4]. Figure 2 shows the energy flow distributions for inner ECAL section before and after smoothing procedure. Calibration constants REF_{ij} for each calorimeter channel were obtained as a ratio of energies in corresponding cells of these distributions. The precision of described algorithm is well illustrated with a distribution of residuals (RMC_{ij} - REF_{ij}) fitted with Gaussian as shown in Figure 3. The initial $\pm 30\%$ uncertainty in relative calibration can be decreased by a factor of $\sim$7 with experimental data collected in very few seconds of data taking. A subset of calorimeter modules calibrated at test beam can considerably improve the performance. It is important to stress that we have not used the known MC shape of energy flow distributions in our analysis. Another important feature of the described procedure is a fact that it uses ECAL information only and therefore it could be used immediately after the LHCb start of data taking.

The results obtained with this method are rather sensitive to the correct pedestal determination as most often we are summing very low energy depositions. However, this problem could be solved by applying some threshold for the signal in a cell to be summed. This will certainly increase the required time which seems not to be a problem.

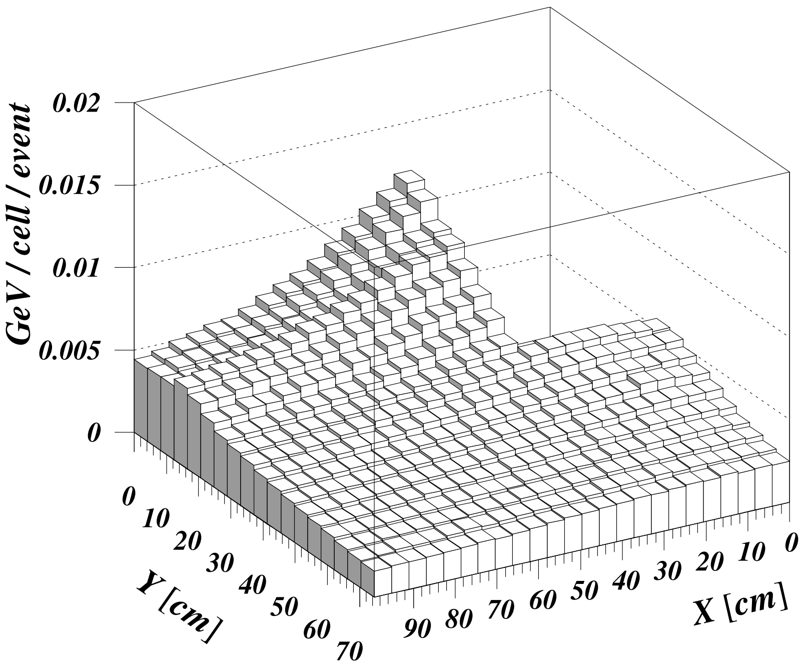

Figure 1: Transverse energy flow distribution normalized to one $b\bar{b}$ event for the lower-left quadrant of inner ECAL section.

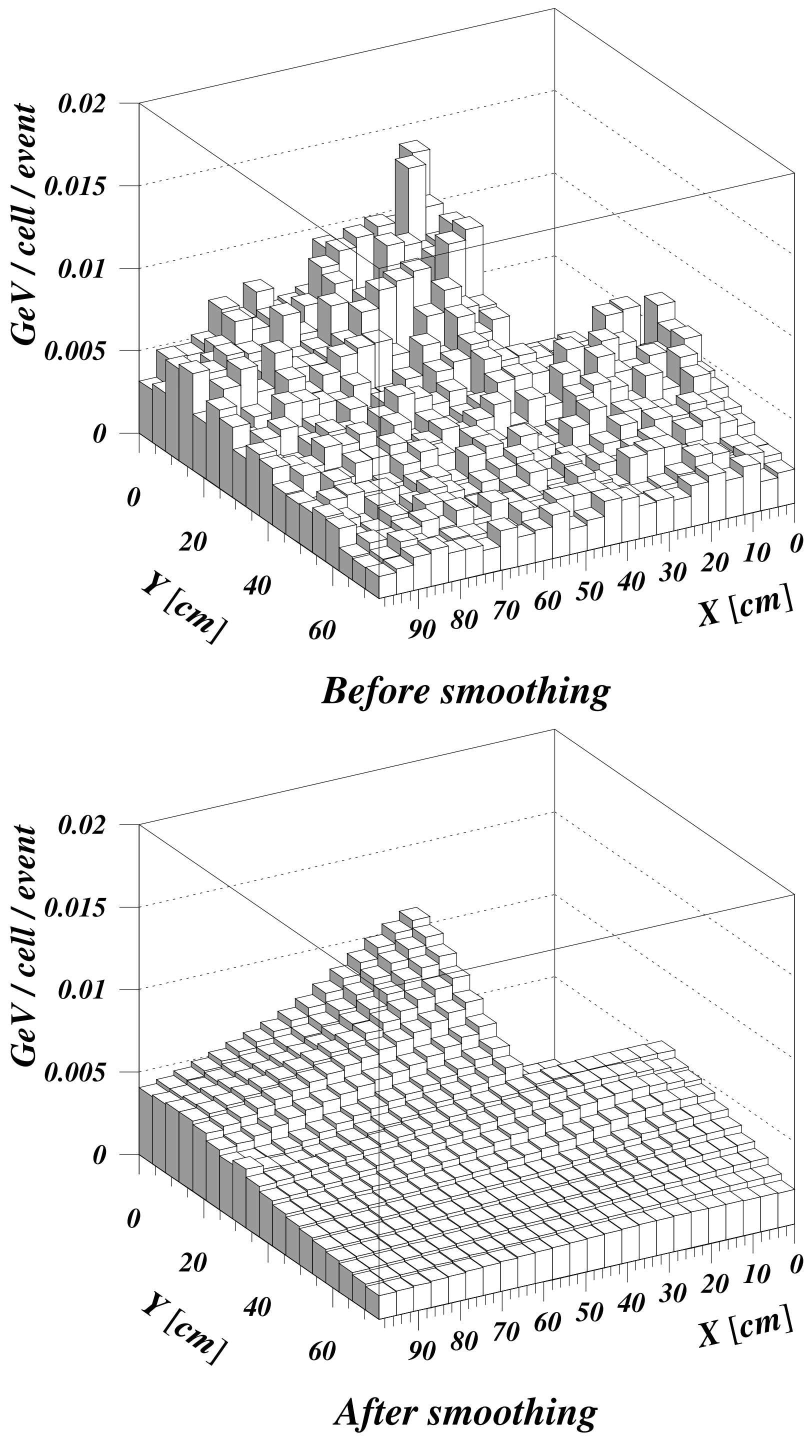

Figure 2: Transverse energy flow distributions for lower-left quadrant of inner ECAL section before and after smoothing.

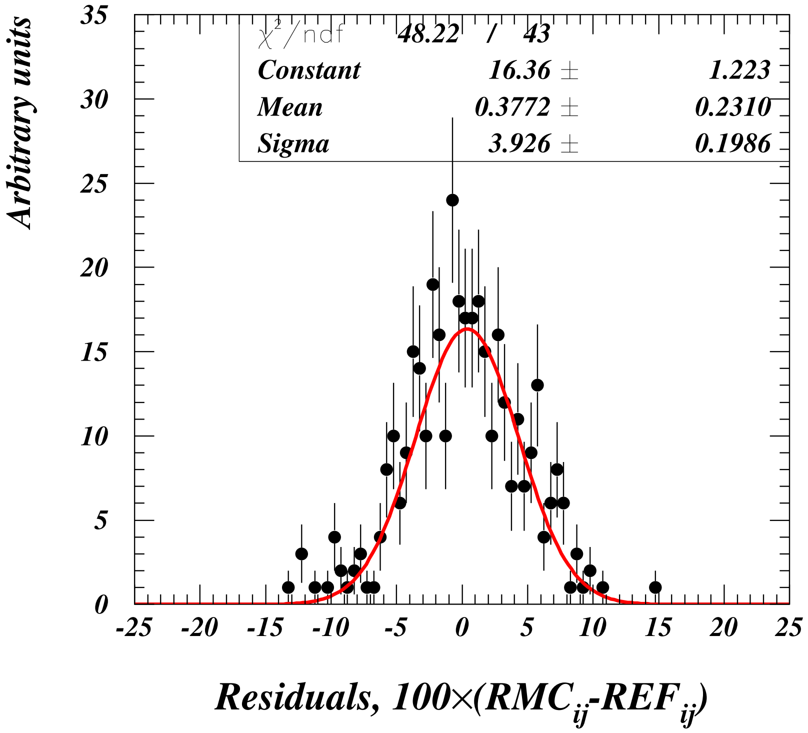

Figure 3: Precision of relative calibration of inner ECAL section with transverse energy flow measurements.

3.2 Monitoring and Calibration with MIPs

As it was already mentioned above the rate of charged hadrons entering the LHCb calorimeter system is high. It depends of course on a distance from the beam pipe as shown in Figure 4 for π mesons with momenta above 2 GeV/c collected in 1 second of the LHCb Level2 trigger operation (40 K events). Many of these hadrons pass through the whole ECAL as a minimum ionising particles, depositing well predictable signal of about 300 MeV . This signal can be used for absolute ECAL calibration at very low energies and for a fast monitoring and control of calorimeter electronics. Most often MIP signals are deposited in one or two neighbour calorimeter cells only which makes the iterative calibration procedure rather simple (fast convergence). MIPs are seen in outer and middle sections of the calorimeter only. In the innermost section ADC bining is too rough.

Outer ECAL section

8	7	12	13	10	6	12	9
22	23	27	26	23	28	20	14
48	57	54	46	47	48	56	43
104	89	98	93	84	94	71	70
107	109	118	111	150	136	135	98
				365	288	232	171
				553	386	270	202

Middle ECAL section

67	65	71	70	54	78	58	54
100	108	118	109	105	110	103	87
				195	160	141	141
				335	266	211	175
				388	310	240	162

Figure 4: Average (per cell) occupancy in the ECAL with π mesons for outer and middle sections. Statistics corresponds to 1 second of data taking at Level2.

It is rather trivial to observe a MIP signal in the electromagnetic calorimeter just counting energy deposited around track entry point. However it requires the information from the tracker which may not be desirable for a fast monitoring and control tool we are discussing in this note. Therefore we have developed algorithm of MIP signal reconstruction using calorimeter information only.

ECAL 3×3 clusters are found requiring the central cell to be the hottest one. Most often (with $\sim$ 70% probability) MIPs deposit energy in two horizontally (due to the magnetic field) adjacent calorimeter cells. Therefore we demand the second most energetic cell to be located to the right or to the left of the cluster center, and energy summed over two hottest cells to be at least 80% of the total cluster energy. Distributions of energy summed over two most energetic cells of the selected clusters are shown in the left column of Figure 5 for outer and middle ECAL sections. A characteristic $\sim$ 320 MeV MIP signal is clearly seen on top of background. The incoherent electronic noise equivalent to one ADC channel was added at the digitisation step of simulation program.

Charged hadrons passing through the ECAL deposit their energy in hadron calorimeter. Requiring a non-zero energy deposition in the HCAL cell just behind the reconstructed ECAL cluster we are able to reduce considerably the low energy electromagnetic background with almost 90% efficiency for the MIPs as illustrated with a right column of Figure 5.

Fitting the central part of the peak with a Gaussian (as shown in Figure 5) we have found the energy resolution of ECAL for the MIPs to be $\sim 12\%$ and $\sim 18\%$ for outer and middle sections correspondingly. Statistics of 1000 MIPs collected per one calorimeter cell would certainly be enough to determine the peak position with MeV accuracy. This statistics could be accumulated in 1000 seconds of data taking at Level2 for the least populated ECAL cells.

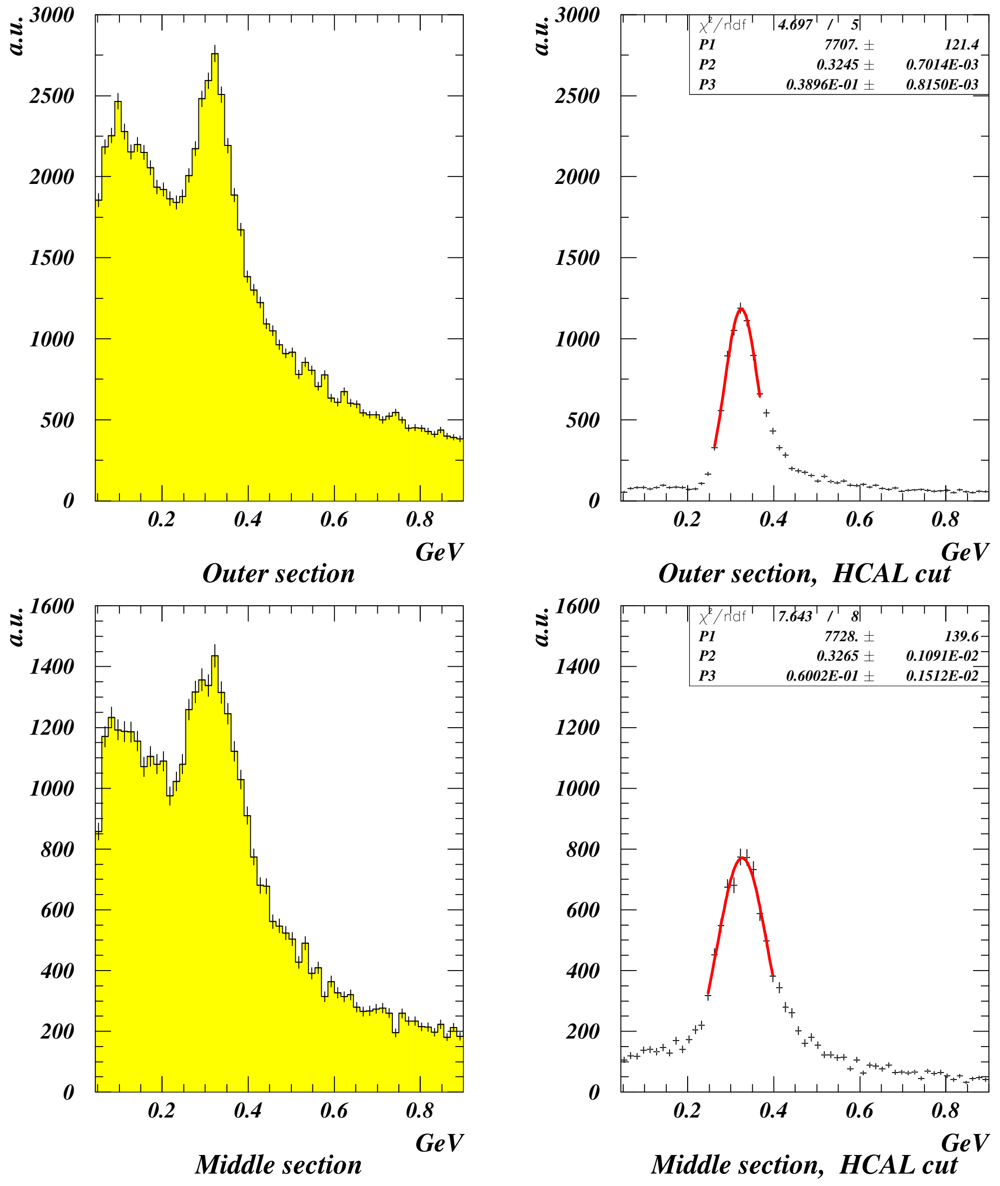

Figure 5: MIPs reconstructed in the electromagnetic calorimeter.

3.3 Calibration with electrons

The most precise calibration of the LHCb calorimeter could be obtained comparing the momentum of electrons (positrons) with energy deposition observed in the corresponding ECAL cluster. Electrons are largely produced by photons converting on a material in front of the magnet. Figure 6 illustrates the population of ECAL with electrons ($E_t > 0.4 GeV/c$) reconstructed by the tracker in 10 seconds of data taking at Level2. The momentum spectra of these electrons are shown in Figure 7.

Outer ECAL section

3	5	4	7	3	8	7	5
15	14	16	16	15	16	16	11
28	27	32	29	38	36	29	32
51	50	62	67	74	77	66	62
35	52	47	47	100	95	95	95
				339	293	273	249
				2013	1686	1554	1379

Middle ECAL section

20	19	25	23	28	29	36	33
40	38	46	53	55	64	70	63
				99	123	113	105
				393	422	402	374
				824	853	829	746

Inner ECAL section

27	35	41	51
45	89	148	128
	146	298	299

Figure 6: Average (per cell) occupancy in the ECAL with electrons (positrons) for outer, middle and inner sections. Statistics corresponds to 10 seconds of data taking at Level2.

The calibration algorithm starts from determination of track entry point to the calorimeter. Then we have performed a search for the closest 3×3 ECAL cluster to the hottest cell in the centre. The flux of hadrons which is much more higher was suppressed with Preshower, requiring an energy deposition above 2 MIPs in the corresponding central cell. For tracks passing this selection we have built an E/p ratio as shown in Figure 8 for perfectly calibrated ECAL. Electrons produce a clear peak around unity. The left wing of E/p distributions comes from hadrons which do not deposit their full energy in ECAL,

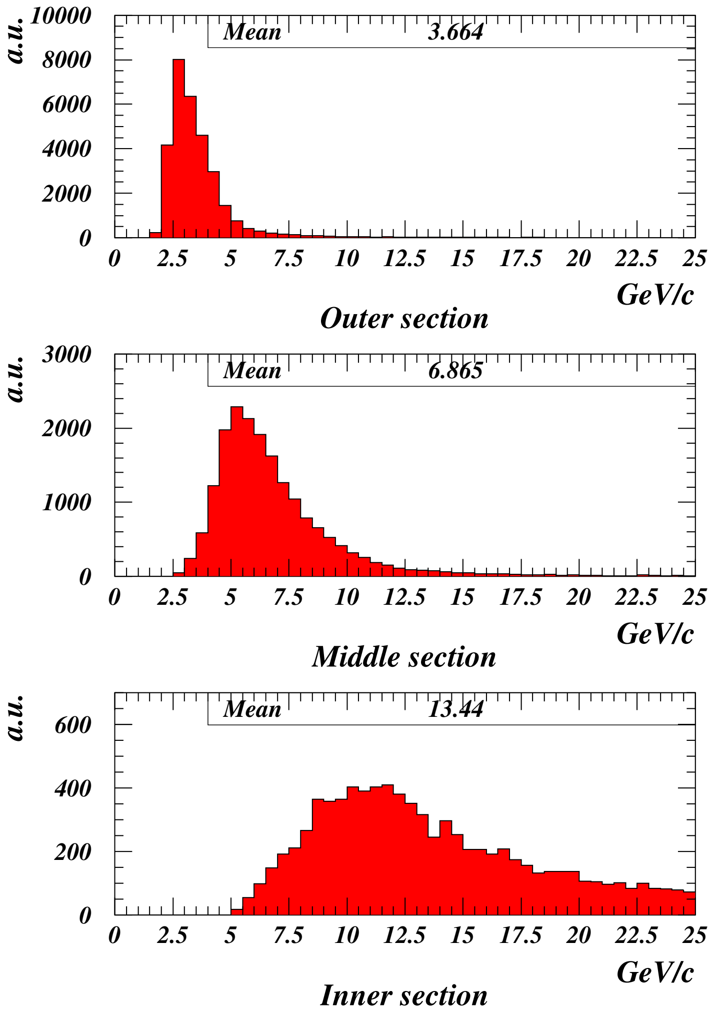

Figure 7: Electron momentum distributions for outer, middle and inner ECAL sections.

while the right tail is explained by pile-up from neighbour particles. The peaks were fitted with a Gaussian.

The calibration of ECAL in real experimental environment is an iterative procedure. Energy depositions in cells of found cluster multiplied with corresponding calibration coefficients are summed and the result is given for the hottest (central) cluster cell. It is then compared with a momentum measured in tracker adjusting the calibration coefficient of central hottest cell to move the electron peak to one. The same algorithm is applied for all other calorimeter cells. Repeating the whole procedure several times we successively improve the calibration. Special hardware (CPUs) should be foreseen at Level2 to fulfil this task.

Within one hour of data taking at Level2 trigger we are able to accumulate ~ 2000 electrons per calorimeter cell even in the least populated region of outer section. This amount of data would allow us to calibrate our detector with a precision by factor 10 better than intrinsic "shashlik" resolution for given energy range.

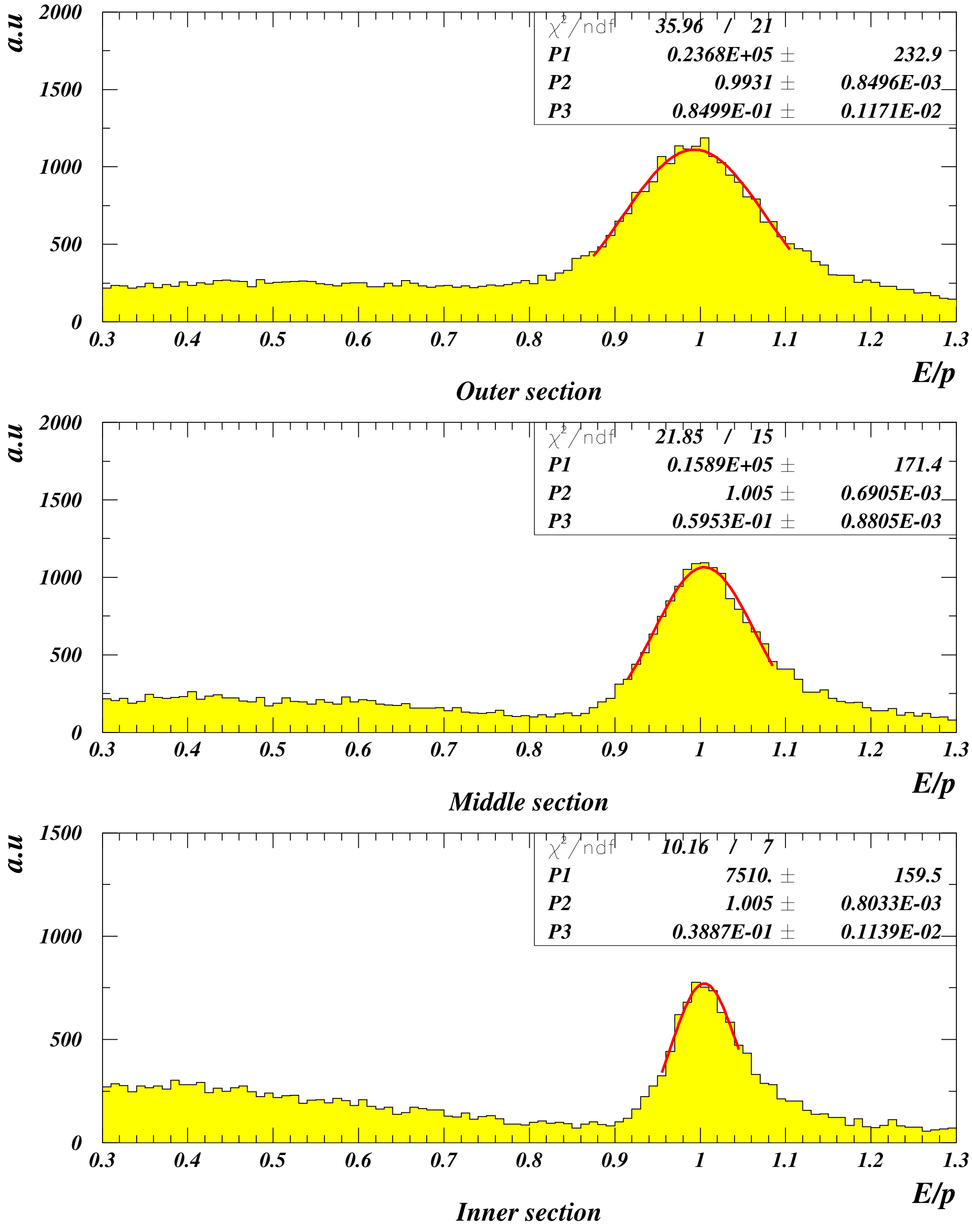

Figure 8: The ratio of energy reconstructed in ECAL to the momentum measured in tracker (E/p ratio) for particles entering outer, middle and inner calorimeter sections.

3.4 Calibration with π^0s

For the very first days of the LHCb operation we foresee the possibility to calibrate calorimeter with π^0signal. The advantage of this method is that it does not require additional information from other LHCb sub-systems. The details of the procedure could be found in HERA-b note [5]. Figure 9 illustrates the π^0peak seen on top of combinatorial background. All ECAL clusters with transverse momentum greater than 0.2 GeV/c were used to construct a signal.

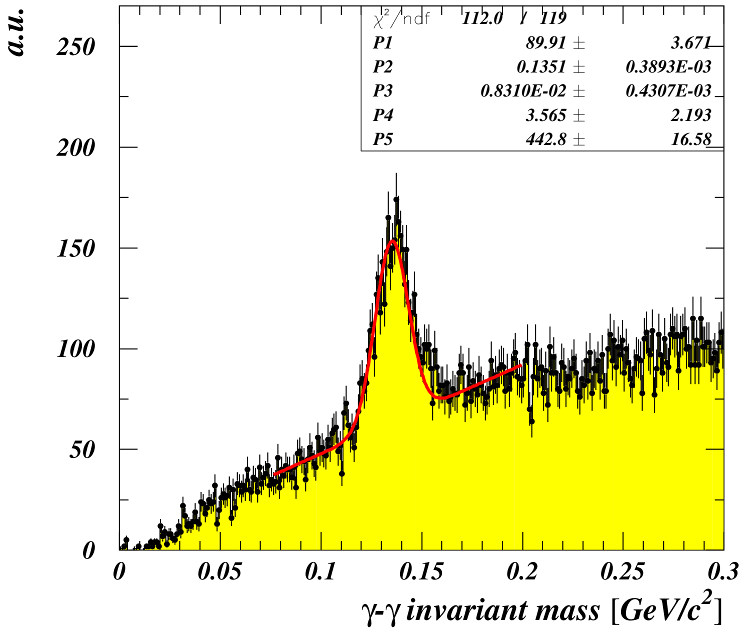

Figure 9: The invariant mass of 2 ECAL clusters (with $E_t > 0.2 GeV/c$).

4 HCAL calibration

The events with inclusive B production generated with SICB were used for these studies. Level-2 trigger routine was applied to the data to simulate the real experimental conditions. This corresponds to the scenario when the calibration procedure is switched on after the Level-2 trigger and , as a consequence, can use the calculated momenta of the tracks, particle identification etc. The following steps were performed to select charged tracks which were then used for the HCAL calibration:

- The momentum $P > 10$ GeV. This is a reasonable cut, since the lowest momentum which can provide the HCAL E_T trigger is about 17 GeV.

- The total energy deposited in the corresponding 3×3 ECAL matrix is less than 0.6 GeV.

To explain this selection criteria Fig.10 shows the energy in the 3×3 ECAL matrix around the track, the left picture of Fig.10 corresponds to the inner region of the calorimeter ($40cm < |x|, |y| < 211$ cm), and the right one to the complementary outer part. The clear signal from the MIP is seen. The background under MIP is ,of course, higher in the inner region due to much higher probabilities to have overlaping showers. The cut $E_{3\times3} < 0.6$ GeV selects MIP's in ECAL, i.e hadrons which deposit the energy in the HCAL(μ's are also selected by this cut). The cut also works automatically as an 'isolation' criteria. We observe about 1.6 of such MIP's per event.

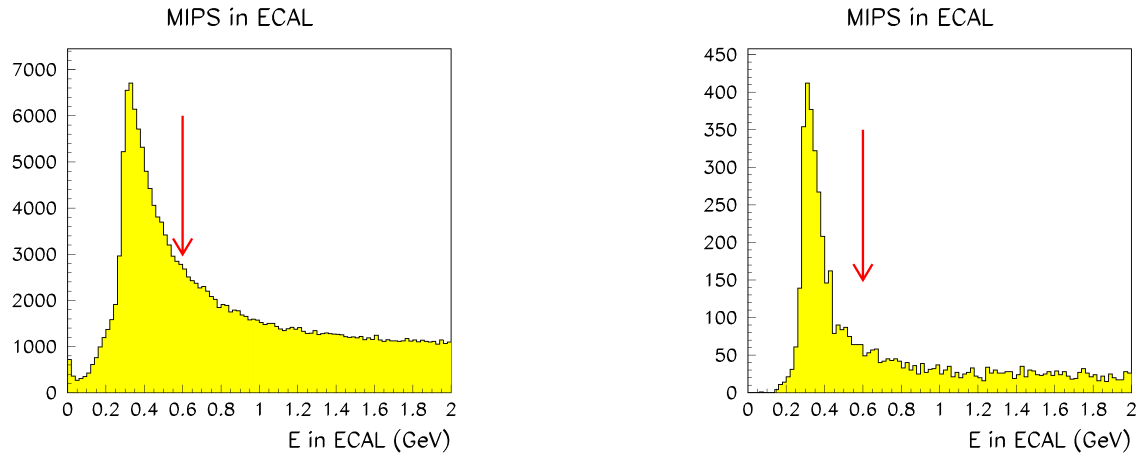

Figure 10: The total energy in the 3 × 3 cluster in ECAL around a charged track

Fig.11 shows the average number of such MIP's/cell in different zones of the calorimeter for total number of 40K events, i.e for 1sec(8sec) of the setup operation if the procedure works at Level-2 input(output).

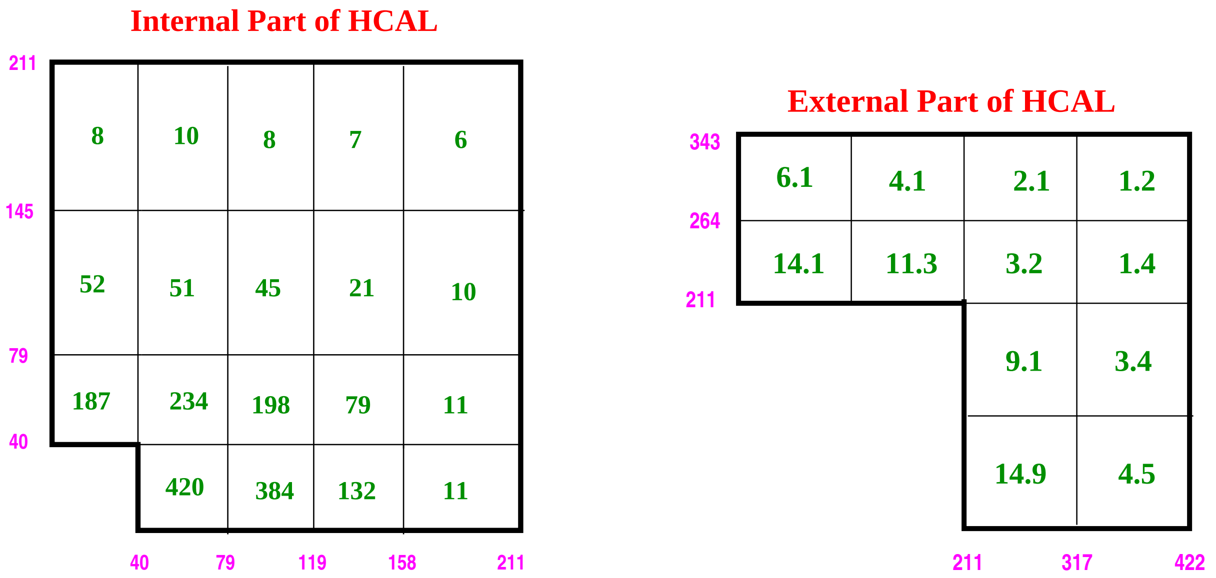

Figure 11: Average(per cell) occupancy in the HCAL with $p > 10$ GeV particles which behave like isolated MIP's in ECAL, the numbers correspond to the total of 40K events, i.e 1 sec. of LHCB data flow after Level-1 trigger.

Fig.12 presents the difference between the energy in the corresponding 3×3 HCAL cluster around the selected track and the particle energy. Clear peak is seen both in inner and outer regions. No special HCAL selections are necessary.

Several algorithm's can be envisaged for the calibration of the calorimeter when a clear peak as in Fig.12 is present as the response of the calorimeter to the particle with known energy. The most 'principle' one is, of course, the minimisation of the sum:

$$\sum_{i,j} \left(\frac{c_i \times a_{ij} - E_j}{E_j}\right)^2$$

Here c_i is a desired calibration coefficient for the i^{th} cell; a_{ij} is the response in the i^{th} cell in j^{th} event; E_j is (known) energy of the incoming particle.

This procedure is certainly suitable for the calibration after the Level-3 when a full modern computer resources are available. It requires a storage space for a large amount of data and is basically slow. As we are working in the context of the Level-2 trigger, it is reasonable to test a much simpler algorithm which does not require accumulation of the data.

We found an example of an algorithm used by GAMS collaboration [6]: Defining

$$E_{ij} = c_i^{old} \times a_{ij}/E_p; E_j = \sum_{i,a_{ij}\neq 0} E_{ij}; w_{ij} = \left(\frac{Eij}{E_j}\right)^{\alpha}; w_i = \sum_j w_{ij}$$

Where c_i^{old} is the initial set of the calibration constants; α is a free parameter, we can assume $\alpha = 2$, for example. Then for the new set c_i^{new} of the calibration coefficients we

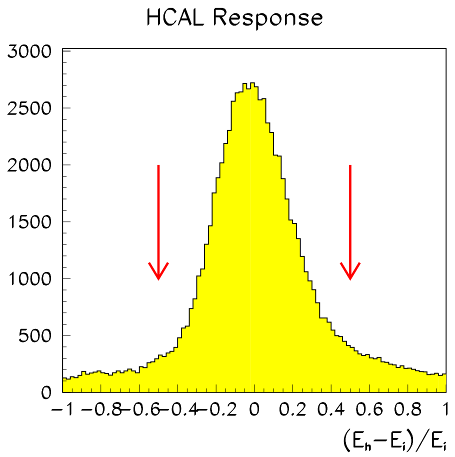

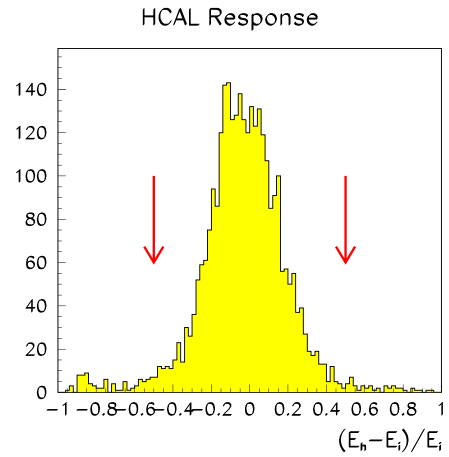

Figure 12: Average(per cell) occupancy in the HCAL with $p > 10$ GeV particles which behave like isolated MIP's in ECAL, the numbers correspond to the total of 40K events, i.e 1 sec. of LHCB data flow after Level-1 trigger.

get:

$$c_i^{new} = c_i^{old} \times (1 + (1 - E_j) \times \frac{w_{ij}}{w_i})$$

Here E_p is the known particle momentum.

To test the convergency speed of the algorithm with a limited number of MC events, the internal part of the calorimeter was reduced to 7×7 matrix. The initial coefficients were uniformelly distributed in the range .5-1.5. Fig.13 shows the results of the tests. It is seen that after ~ 5000 events per cell the dispersion of the coefficients distribution becomes $< 1\%$, which is enough for the HCAL calibration.

5 Conclusion

The present study demonstrated the feasibility of *in situ* calibration of the LHCB calorimeters. For the case of the HCAL it is proved that ~ 5000 events is enough to achieve 1% accuracy. To achieve such a statistics in the peripheral cells of the HCAL about ~ 5000 sec of LHCB data flow after Level-1 trigger is sufficient. More conservative assumption, i.e the start of the calibration after Level-2 results in ~ 10 hours to achieve the same accuracy.

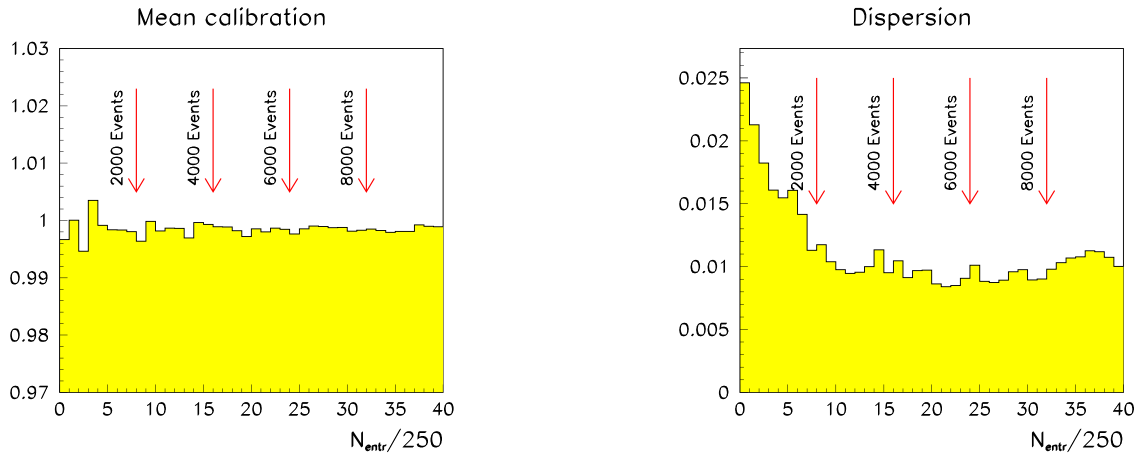

Figure 13: Results of the convergency tests of the calibration algorithm a) shows the evolution of one of the coefficients; b) shows the evolution of the rms of the distribution of 5×5 coefficients.

References

[1] LHCb Technical Proposal, CERN/LHCC 98-4, LHCC/P4, Feb. 1998.

[2] LHCb 2000-028, The Front-End Electronics for LHCb calorimeters

[3] LHCb 2000-043, Design and construction of electromagnetic calorimeter for LHCb experiment, public note.

[4] J.Allison, Multiquadratic Radial Basis Functions for Representing Multidimensional High Energy Physics Data, Comp. Phys. Comm., 77:219, 1993.

[5] Online π^0 calibration of ECAL, HERA-B internal note.

[6] A.Lednev, O.Tchikilev Private communication.